IMEKO International Conference on
Metrology for Archaeology and Cultural Heritage
Torino, Italy, October 19-21, 2016

High efficiency Raman system for safe molecular characterisation of pigments

Andrea Azelio Mencaglia, Iacopo Osticioli, Salvatore Siano*

*Istituto di Fisica Applicata "N.Carrara"-Consiglio Nazionale delle Ricerche, Via Madonna del Piano 10, 50019 Sesto Fiorentino, Italy. *) E-mail: S.Siano@ifac.cnr.it*

***Abstract* – An innovative portable Raman system (exc. wav. 1064 nm) for safe molecular characterisation of pigments and other photosensitive materials has been developed and successfully tested. It was equipped with a novel probe, which has been designed and built in order to perform Raman scattering measurements on a relatively large area homogeneously irradiated at laser intensities lower than the typical ones needed using commercial instruments. Besides a set of original optical solutions providing improved efficiency, the instrument has also been equipped with an active thermal control line, which allows to prevent alterations of the material under study and to optimize the measurement cycles by means of suitable modulations of the laser power. Comparative tests of the novel analytical tool with an alternative setup equipped with a commercial Raman probe were carried out on a set of pure pigments and oil paint layers, which allowed assessing the higher measurement efficiency and reliability of the former with respect to the latter.**

I. INTRODUCTION

Along the last two decades, the application of Raman spectroscopy in archaeometry and conservation of cultural heritage, as well as in other fields, has undergone significant technological and applicative advances. Nowadays, this vibrational technique along with its complementary one (FT-IR) represent the most used approaches for the molecular identification of pigments, binders, and alteration materials of a large variety of artefacts. Furthermore, Raman spectroscopy has also been exploited for characterising the effectiveness of conservation treatments, such as those based on laser ablation [1]. This widespread use has been mainly favoured by the significant technological developments of the solid state lasers and optical components, along with the miniaturisation of the detectors, associated electronics, and personal computers. These technological trend have allowed significant size and cost reductions of the Analytical instruments and the development of portable devices [2] with spectral resolutions and signal to noise responses not far from those of the laboratory instruments.

Raman spectroscopy is usually referred to as a non-destructive technique although such a safe condition can be achieved only through careful optimisation of the irradiation parameters, or more often by operating at low intensities. However, when the measurement time need to be reduced in order to make a number of consecutive measurements and the objects of cultural interest to be analysed include paint layers, organic fibres, plastics, and other, the achievement of safe measurement conditions can be rather difficult because of the high photosensitivity and low critical thresholds of these materials. The excitation wavelength of 1064 nm is often preferable because of the strong fluorescence of organic materials at lower wavelengths (exc. 785 nm or lower). Anyway, because of the high intensities usually needed, the mentioned materials can easily undergo photothermal/chemical damages, such as discoloration, redox reaction, and/ ablation, with unacceptable visible alterations of the artefact under analysis. Furthermore, the operative conditions can become very critical whenever highly absorbing endogenous and/or exogenous materials are encountered. Such an injury risk also represents a severe obstacle to the repeatability and reliability of the measurements and then to the possibility to implement automated compositional mapping and line-scanning Raman imaging.

In the present work, the development and comparative testing of an innovative Raman system (exc. wav. 1064 nm) is reported. The instrument was equipped with an optical set up allowing to operate with a relatively large laser spot along with automated energy release to the target driven by online temperature monitoring. We recently reported the basic idea of the temperature control [3], its working principle and technical details [4]. Besides the improvement of the system, here, we focus on the its technical solutions and extensive comparison with an alternative setup equipped with a commercial Raman probe. The results achieved show the significant advantages of the novel analytical system in view of efficient Raman mapping of polychrome surfaces, such as those of paintings [5-6], stones, and other.

II. TECHNOLOGY AND METHODS

The novel Raman system (system A in the following)

including excitation source, probe, thermal control line, spectrometer, fibre coupling, and software was designed and built according to the following component design.

- 500 mW diode-pumped Nd:YAG (1064 nm) excitation laser beam, which was homogenised via optical fibre or diffractive optics and then focused in a spot diameter of 0.45 mm. In the former case (fibre core diameter: 200 µm) the maximum power release to the target was 280 mW.
- Reflective optics with a high numerical aperture (about 0.4) for efficient collection of the scattered radiation;
- Laser power feedback loop for preventing overheating based on the continuous measurement of the temperature of the irradiated spot using an IR thermopile sensor.
- Precise positioning and visual monitoring using LED aiming beams and a CCD camera.
- IR spectrometer equipped with a 512-pixel deep-cooled (-60°C) InGaAs array detector and a monochromator covering the spectral range between 165-1825 cm^{-1} with a resolution of 8 cm^{-1}. (BaySpec Inc., CA, USA), which was thermally stabilized in order to reduce the fluctuation of the thermal background.
- Maximising the optical coupling between the reflective collector and the sensor array of the spectrometer using a suitable fibre bundle.
- Driver and applicative software allowing for full control of the operating conditions, data acquisition, management, and display.

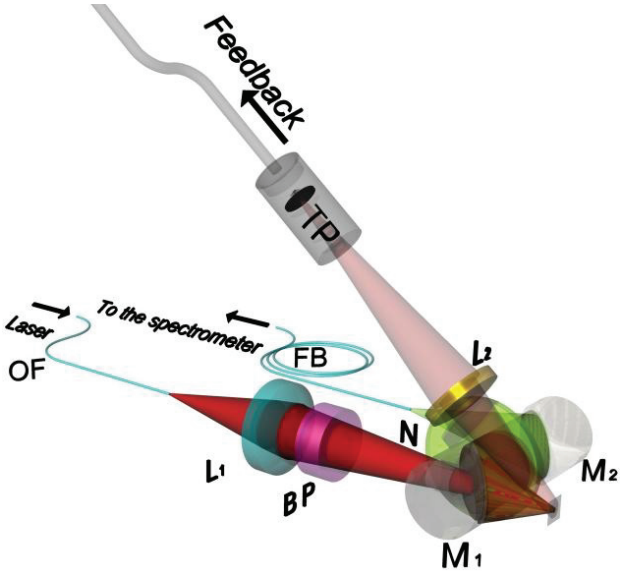

Figure 1 - Schematic set up of the innovative probe of the Raman system A. $L_{1\text{-}2}$: lenses; $M_{1\text{-}2}$: 90° off-axis parabolic mirrors; BP and N: bandpass and notch filter, respectively. TP: thermopile.

In Fig. 1, a schematic setup of the novel probe and of its fibre-couplings to the laser source and the spectrometer and the mentioned component implementations are displayed. As shown, the DP Nd:YAG(1064 nm) laser was coupled to a hard clad silica (HCS) optical fibre (OF), 200/230 µm core/clad; the fibre output was imaged onto the sample by means of an aspheric lens, L_1 (f=18.75 mm); the 2.25× magnification configuration produced a top-hat spot of 450 µm diameter. A 10 nm wide bandpass filter, BP, centred at 1064 nm was placed after the lens L_1 in order to cut-off the fibre's Raman scattering contribution. The optical collector was achieved using a pair of off-axis, 90°, parabolic mirrors, ½ inch diameter. The primary one, M_1, which was drilled in order to let the laser beam pass through, had a focal length of 15 mm (NA: 0.41) while that of the secondary one, M_2, was 25.4 mm. The latter was selected in order to better match the numerical aperture of the fibre coupling to the spectrometer, which was assessed through signal efficiency measurement by comparing different fibre and bundles. The best results were provided by a fibre bundle with seven fibres (ϕ 105/125 µm core/clad, NA = 0.22), packed circularly at the input tip (collector side) and linearly at the output one (spectrometer side), which was aligned along the direction of entrance slit. The notch filter (N) centred @ 1064 nm, 44 nm-wide blocking window (OD > 6) for rejecting the elastic scattering component, was placed between the two mirrors.

The thermopile sensor (TP) was calibrated according to a corrected blackbody emission formula and the direct measurement of the emissivity of the target in order to provide the temperature evolution *T(t)* at the irradiated area, which was imaged on the sensor by means of the ZnSe lens, L_2 (see [2] for further details). *T(t)* was used as input observable of the power control *P(t)* with Proportional-Integral (PI) feedback:

$$P(t) = \begin{cases} B \cdot \Delta T(t)^{\frac{1}{5}} \tanh\left(\frac{t}{\tau}\right) + C \cdot \int_0^t \Delta T(t')^{\frac{1}{5}}\, dt', & \Delta T(t) > 0 \\ P_{min}, & \Delta T(t) \le 0 \end{cases} \quad (1)$$

where $\Delta T(t) = T_{set} - T(t)$, B, C and τ are adjustable parameters, T_{set} is the expected temperature set by the operator, and P_{min} was set at 20 mW (arbitrary value selected in order to avoid the switch-off of the laser when deep power modulations were induced by rapid temperature rises).

The suitable selection of the B, C and τ parameters allowed optimizing the laser energy release to the target in order to avoid undesired overheating and alteration of the sample under analysis. In some details τ = 0.7 s guaranteed a gradual power increase during the onset phase, which was needed in order to avoid to high thermal gradients within the response time of the thermopile, TP, (1.3 s). B can assume values ranging

between 2.8-28 mW°C$^{-1/5}$, while C ranges between 8.4·10^{-3}- 42·10^{-3} mW°C$^{-1/5}$s^{-1}.

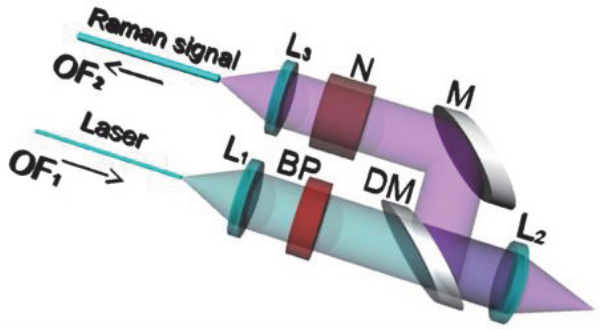

Figure 2 - Schematic set up of the commercial probe used in the Raman system B. $L_{1\text{-}3}$: lenses; DM and M: dichroic mirror and flat mirror, respectively; BP and N: band pass and notch filter, respectively.

The performance of the described Raman system A were compared with those of an alternative setup (system B) achieved using the same laser excitation source and spectrometer of the system A and the commercial probe schematised in Fig. 2. In this second case, the scattered light was collected and collimated by the same lens, L_2 (NA= 0.4) used for focusing the laser beam (focal spot diameter of 105 µm), extracted from the incidence optical axis by means of a dichroic mirror (DM), bent using a flat mirror (M), filtered (N), coupled to the optical fibre (200 µm core diameter), and eventually sent to the spectrometer.

The comparison between the two systems was carried out by considering the following exposure-normalised detection efficiency parameter:

$$\mathcal{E} = \frac{I_{max}}{\int_0^{t_L} I_L\,(t)dt} = \frac{I_{max}}{F_{tot}} = \left[\frac{counts}{J/cm^2}\right], \qquad (2)$$

where I_{max} is the peak intensity of the Raman band (after baseline subtraction) selected for comparison, I_L the laser intensity, t_L the irradiation time, and F_{tot} the total radiant exposure at the focal laser spot. Alternatively, the detection performances can be compared by considering counts/sec at a fixed laser intensity.

III. RESULTS AND DISCUSSION

Extensive measurement tests have been carried out on a set of mercury, copper and iron based pigment samples using both the Raman systems described above.

Such a comparison pointed out the detection efficiency of the system A was significantly higher than that of the system B. Thus for example, as shown in Fig. 3, for cinnabar (HgS), a similar maximum of the most intense band at 252 cm^{-1} was achieved with the system A using much lower intensity and radiant exposure than those needed for the system B. The corresponding efficiency parameters (Eq. 2) were: ε_A= 186 counts·cm^2/J, ε_B=12 counts·cm^2/J. For both spectra the acquisition time was t_{LA}=t_{LB}=3 s.

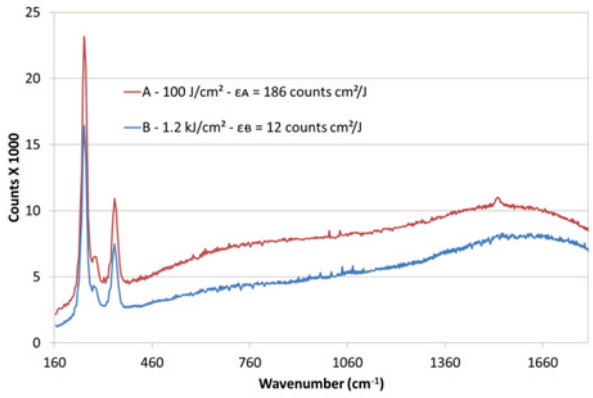

Figure 3 - Raman spectra of cinnabar collected using the system A (red line) and the system B (blue line), respectively, using different irradiation parameters.

The signal improvement achieved has to be attributed to the following main features of the novel system (A): 1) larger laser spot (450 against 105 µm) with a top-hat energy distribution produced by the single lens (L_1 in Fig. 1) imaging configuration; 2) overall improvement of the optical collection setup thank to the use of the fibre bundle FB (Fig. 1) with the mentioned asymmetric packing, which allowed collecting more light from the irradiated spot and better exploit the active area of the sensor array of the spectrometer.

In all the cases, the acquisition time can be reduced by increasing the excitation intensity, according to the linear dependence of the Raman scattering on the latter within the linear range. However, the irradiation parameters should not overcome the alteration threshold of the material under study.

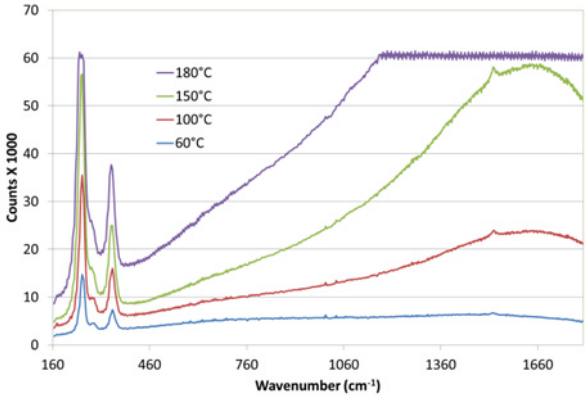

Figure 4 - Spectra of cinnabar achieved at almost constant temperatures with the PI feedback control loop activated. The drastic increase of the continuum

component was observed at 180 °C, in proximity of the permanent alteration of the sample.

The present configuration of the system A allowed a maximum intensity release to the target of about 180 W/cm^2. A permanent darkening of cinnabar was observed after about 3 s at 100 W/cm^2, which corresponded to a peak temperature of 188°C (Fig. 4) detected by the thermopile. Conversely, alteration of cinnabar using the system B was observed after a similar irradiation time at 600 W/cm^2. Such a significant difference between the two alteration thresholds has to be attributed to the different spot diameters and beam distributions of the two systems.

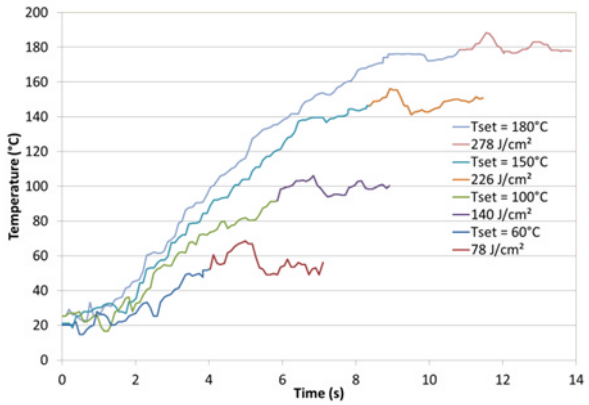

Figure 5 - T(t) profiles for several values of T_{set} with the PI feedback control loop activated (Eq. 1). Spectra of Fig. 4 were achieved during the last 3 s of each profile, with the exposure values reported in legend.

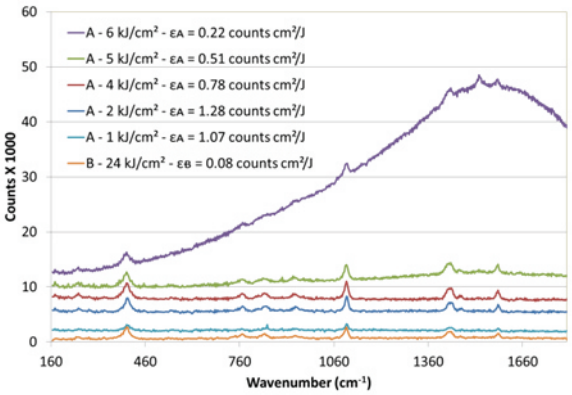

Fig. 6 – Azurite Raman spectra obtained with the systems A and B at different exposure conditions (60 s integration time); the respective efficiencies evaluated for the peak at 1100 cm^{-1} are reported.

In order to safely expose the sample, the system A allowed to activate the PI feedback control loop according to Eq. (1). It was then possible to start the spectrum detection either soon after the laser was switched ON, or when the surface temperature of the target approached the T_{set} value within a certain ΔT. Thus for example in Fig. 4, several spectra of cinnabar are shown, which were achieved using 3 s integration time, by starting the acquisition only when the target temperature was close to T_{set} (ΔT=T-T_{set}=–2°C). The respective temperature time profiles are reported in Fig. 5, where the last 3 s, during which the spectra have been collected, are highlighted.

Thus, in view of Raman scan of relatively large areas the system A and associated optical solutions offer the possibility to significantly reduce the acquisition time by preventing undesired alterations of the sample. In particular, Fig. 4 shows that safe spectral analysis of cinnabar can be carried out up to a surface temperature set around 150 °C, which corresponds to the maximal practicable acquisition speed on the present sample (down to a fraction of second in order to achieve several thousand counts).

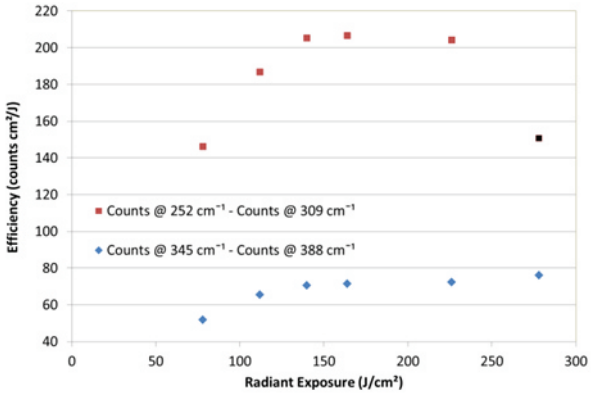

Figure 7 - Cinnabar: detection efficiency of cinnabar peaks @ 252 and 345 cm^{-1} vs radiant exposure

Similar tests were carried out on azurite, $Cu_3(CO_3)_2(OH)_2$, which exhibited a permanent darkening at a laser intensity of about 120 W/cm^2, close to that of cinnabar. Also in this case the efficiency (which was in general lower than for cinnabar) of the system A was significantly higher than that of the system B. The former, which was calculated in different irradiation conditions, showed a pronounced dependence on the radiant exposure: ε_A=0.22-1.28 for radiant exposures between 1-6 kJ/cm^2 and the maximum efficiency was achieved at 2 kJ/cm^2. Such a peaked behaviour of ε_A, which was observed also for cinnabar (252 cm^{-1} band in Fig. 4), could perhaps be related to the possible reversible variation of the optical parameters of the pigment under irradiation at increasing laser intensities and total radiant exposure. In view of future substantial systematic insights on this feature, where both the dependences on total fluence and intensity must be investigated, let also observe that the examination of the intensities of the main

band of cinnabar at 252 cm^{-1} exhibited different efficiency behaviour with respect to that at 345 cm^{-1}. As shown in Fig. 7, the former was saturating towards a maximal value of about 80 counts cm^2/J).

Spectral analyses were finally carried out on hematite pure pigment and a red ochre paint layer in linseed matrix applied on a gypsum and rabbit glue preparation of a wooden panel. As shown in Fig. 8, reporting some of the Raman spectra collected after baseline subtraction, intermediate efficiencies between those of cinnabar and azurite were found and the system A confirmed its superior performance.

Very interestingly, the Raman signal of the paint layer was significantly higher than that of pure pigment powder. The best exposure-normalised efficiency (ε_A= 2.32 counts·cm^2/J as calculated by considering the band at about 290 cm^{-1}) was found at 350 J/cm^2 (orange), whereas a saturation effect was observed at about 1 kJ/cm^2 (pink). The main bands of red ochre and underlying gypsum preparation were clearly recognisable in the spectrum corresponding to the former condition, which was collected in 10 s using a laser intensity of 35 W/cm^2. The observed intensities of the Raman bands suggest that a slightly higher intensity and shorter acquisition time (ex. 5 s) could be used in scanning operative conditions.

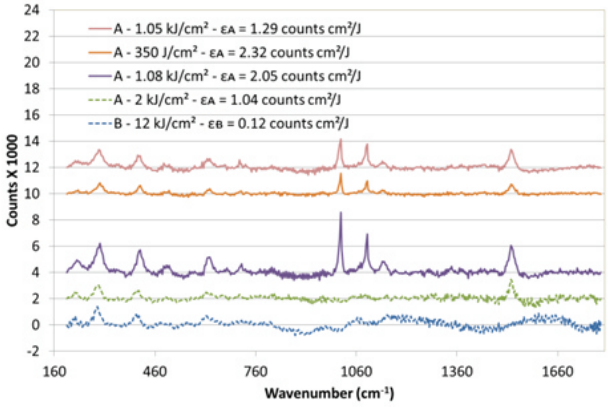

Figure 8 - Spectra of hematite pure pigment (two dotted spectra at the bottom) and of red ochre paint layer (three solid spectra) as measured using the systems A and B, respectively, and different irradiation parameters. The detection efficiency, ε, refers to the band at 290 cm^{-1}.

IV. CONCLUSIONS

An innovative Raman system implementing a novel probe and equipped with a thermal control line for investigating the temperature dependence and preventing undesired alterations of the material under analysis has been developed. The comparison of its performances with those of an alternative system including a commercial Raman probe evidenced the significant advantages of the novel instrument.

The tests were carried out on pure pigments and a red ochre paint layer and the comparison of the instrumental detection efficiency carried out using an exposure-normalised efficiency parameter. This showed in general an improved signal optical collection and detection of the novel system, which allow to operate at lower intensities and temperatures of the usual ones, as well as to reduce the measurement times. These features are very promising in order to develop an efficient Raman scanner able to provide automated molecular mapping of valuable polychrome surfaces without relevant risks of material alterations.

We are currently extending the present work through further technical improvements, comparisons of performances using different detection efficiency parameters, extensive application tests on a set of paint layers, and determination of optimised operative conditions.

ACKNOWLEDGEMENTS

The present work represents the first step towards the development of a Raman scanner foreseen in the project FOTON*ART* funded by the Ente Cassa del Risparmio di Firenze, while the development of the thermal control was carried out within the activities of the European project IPERION-CH "*Integrated Platform for the European Research Infrastructure on Cultural Heritage*" (H2020-INFRAIA-2014-2015, Grant Agreement n. 654028).

REFERENCES

[1] S. Siano, J. Agresti, I. Cacciari, D. Ciofini, M. Mascalchi · I. Osticioli · A.A. Mencaglia, Laser cleaning in conservation of stone, metal, and painted artifacts: state of the art and new insights on the use of the Nd:YAG lasers, Appl Phys A 106 (2012) 419–446.

[2] P. Vandenabeele, H. G. M. Edwards, J. Jehlička, The role of mobile instrumentation in novel applications of Raman spectroscopy: archaeometry, geosciences, and forensics, Chem. Soc. Rev., 2014,43, 2628-2649.

[3] A. A. Mencaglia, I. Osticioli, S.Siano, optimising raman spectroscopy for Characterising biological growths on stone artefacts, Fotonica AEIT, Italian Conference on Photonics Technologies, IET 2015. DOI: 10.1049/cp.2015.0188.

[4] I. Osticioli, A. A. Mencaglia, and S. Siano Temperature-controlled portable Raman spectroscopy of photothermally sensitive pigments, Sensors and Actuat. B-Chem. 238 (2017) 772–778.

[5] A. Brambilla, I. Osticioli, A. Nevin, D. Comelli, C. D'Andrea, C. Lofrumento, G. Valentini, R. Cubeddu, A remote scanning Raman spectrometer for in situ measurements of works of art, Rev. Sci.

Instrum. 82, (2011) 063109.
[6] S. Mosca, R. Alberti, T. Frizzi, A. Nevin, G. Valentini, D. Comelli, A whole spectroscopic mapping approach for studying the spatial distribution of pigments in paintings, Appl. Phys. A 122 (2016) 815-825.